Schweizerische Mineralogische und Petrographische Mitteilungen 83, 81–96, 2003

Petrology and geochemistry of the Late Jurassic calc-alkaline series associated to Middle Jurassic ophiolites in the South Apuseni Mountains (Romania)

Ionel Nicolae[1] and *Emilio Saccani*[2]

Abstract

In the South Apuseni Mountains (SAM), Romania, Jurassic calc-alkaline magmatic series occur in association with Jurassic ophiolites within a narrow belt that marks the boundary between the Eurasian and Adria Paleozoic continental margins. This association of magmatic series has been previously reported as a single ophiolitic sequence by many authors. Calc-alkaline rocks include volcanic and intrusive rocks and, along with associated ophiolites, occur in a composite nappe system in the central and NE part of the SAM. Volcanic rocks directly overlie ophiolites and include basalts, basaltic andesites, andesites, dacites, and rhyolites, while dykes intrude both calc-alkaline volcanics and ophiolites, and are mainly represented by andesites and dacites, locally showing high-K calc-alkaline affinity. Intrusive rocks mainly include granites and granodiorites.

Geochemical characteristics of the studied rocks correspond to those generated in island arc settings, with a depletion of HFSE relative to LILE, and a marked enrichment of LREE. Mineral–melt exchange equilibria, as well as bulk-rock major and trace element abundances indicate that fractional crystallization in closed systems played a major role in controlling the magmatic evolution of the SAM calc-alkaline series.

Geothermometric and geobarometric estimates indicate that temperature along the fractionation trend varied from 1216 °C for the less evolved rocks down to 860 °C for the more evolved rocks, at pressures between 1.8–2.3 kbar. SAM calc-alkaline lavas were derived from a MORB-like depleted source modified by slab-derived fluids in an intra-oceanic island arc setting that developed during the closure of the Vardar oceanic basin. These island arc series were formed by both intrusion and extrusion of calc-alkaline rocks into and onto a pre-existing oceanic crust now represented by SAM ophiolites. In contrast to some previous interpretations, data presented in this paper demonstrate that no genetic link exists between the calc-alkaline series and the underlying ophiolitic rocks.

Keywords: Calc-alkaline magmatism, petrology, Apuseni Mountains, Romania.

Introduction

The South Apuseni Mountains (SAM) represent a narrow belt that marks the boundary between the Eurasia plate and the Tisza (Austro-Bihorean) microplate, which represent the northernmost edge of the Adria plate (Dal Piaz et al., 1995; Dalmeyer et al., 1999). Late Jurassic calc-alkaline rocks are widespread in the SAM (Fig. 1) and are always associated with Jurassic ophiolites (Savu et al., 1981; Cioflica and Nicolae, 1981; Hovorka, 1996). In particular, calc-alkaline volcanics stratigraphically overlie the ophiolitic sequence, and calc-alkaline granitoids intruded the ophiolites, suggesting that the magmatic activity developed after the emplacement of the ophiolitic sequence.

The tectono-magmatic significance of the calc-alkaline series is controversial, as is the geodynamic significance of their association with ophiolites. Two contrasting models have been proposed. One postulates that calc-alkaline rocks were generated in an intra-oceanic arc where MOR-type ophiolites had previously been emplaced. This model assumes no genetic relationship between calc-alkaline and ophiolitic rocks (Savu et al, 1981; Saccani et al., 2001; Bortolotti et al., 2002). The alternative model suggests that the calc-alkaline series and the ophiolites belong to a single magmatic sequence (e.g., Radulescu and Sandulescu, 1973), with the calc-alkaline representing the evolved products of intra-oceanic island arc activity which began with the generation of the ophiolitic suite (Nicolae, 1995; Cioflica and Nicolae, 1981).

Data so far presented in the literature do not allow a definite interpretation in terms of of these tectono-magmatic models. The purpose of this pa-

[1] Institutul de Geodinamica al Academiei Romane, Bucuresti, Romania.
[2] Dipartimento di Scienze della Terra, Università di Ferrara, I-44100 Ferrara, Italy. <e.saccani@unife.it>

0036-7699/2003/83/81

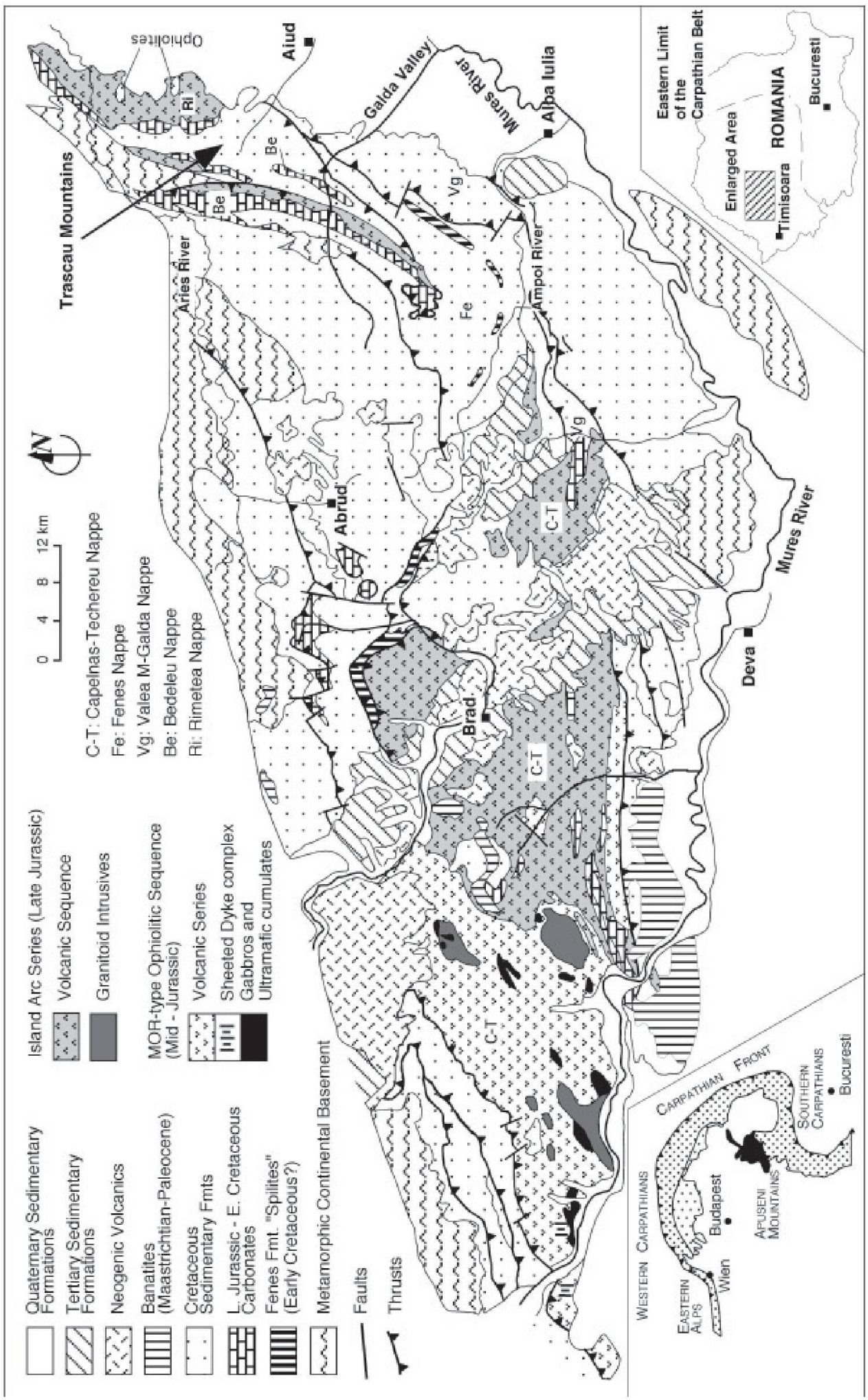

Fig. 1 Simplified geological sketch-map of the South Apuseni Mountains. Modified after Saccani et al. (2001) and references therein. Location of the study area (bottom right) and position of the South Apuseni Mountains with respect to the Carpathian Belt (bottom left) are also shown.

per is to present new data on the mineralogy and whole-rock composition of the SAM Jurassic calc-alkaline series, to constrain the magmatic evolution and define the tectono-magmatic setting of formation.

In addition, since the magmatic series studied in this paper had developed in a collisional setting located at the northernmost border of the Mesozoic Adria-Vardar ocean system, the data presented in this paper may add constraints for the geodynamic reconstruction of this sector of the Vardar oceanic basin and its related continental margins.

Geological setting

The Apuseni Mountains represent a narrow structural belt located in the innermost part of the Southern Carpathian orogenic belt (Fig. 1). They are tectonically subdivided into two main zones: the North Apuseni (Internal Dacides) and the South Apuseni Mountains. The North Apuseni zone consists of a crystalline basement covered by a Permian–Lower Cretaceous sedimentary sequence, and shows general geological features very similar to those of the Austroalpine basement. The SAM mainly consist of a pile of tectonic units known as the Mures nappes complex in which Mesozoic magmatic rocks are widespread (Radulescu and Sandulescu, 1973; Hovorka, 1996; Bortolotti et al., 2002). Among the distinctive features of the SAM is the occurrence of the most widespread Jurassic ophiolitic sequences of the Carpathians and the close association of these with Late Jurassic calc-alkaline magmatic sequences (Nicolae, 1995). In particular, ophiolites and associated calc-alkaline magmatic rocks are found in the Capalnas-Techereu (C-T) Nappe, which surfaces in the central part of SAM, and in the Fenes and Rimetea Nappes, located in the Trascau Mountains (T-M), in the north-easternmost part of SAM (Fig. 1). The Mures complex traces the boundary separating the Paleozoic rocks of the ancient continental margin of the Eurasian plate, to the north, from the Tisza microplate (Kovacs, 1982) possibly representing the northernmost edge of the Adria plate (Dal Piaz et al., 1995). The Apuseni Mountains sector of the Tisza microplate is also known as Pre-Apulian or Foreapulian Zone (Sandulescu and Visarion, 2000). This boundary is interpreted as the record of a Late Jurassic ocean plate convergence which led to a continental collision during the Late Cretaceous. To the south, the Mures complex is separated from the Bucovino-Getic nappes (Marginal Dacides) of the South Carpathians by the Miocene South-Transylvanian fault system. According to Burchfiel (1980) a dextral transpression along this fault displaced the SAM terranes about 300 km eastward. Consequently, their pre-Miocene position was probably in the northern prolongation of the Dinaride belt.

SAM ophiolites are characterised by prevailing volcanic rocks and subordinate mafic and ultramafic intrusive rocks, and originated in a mid-ocean ridge setting (Savu et al., 1994; Saccani et al., 2001; Bortolotti et al., 2002).

Calc-alkaline rocks include a well-developed volcanic sequence, subvolcanic dykes and small granitoid intrusive bodies (Cioflica and Nicolae, 1981; Savu et al., 1996; Hovorka, 1996; Bortolotti et al., 2002). Volcanic rocks directly overlie the ophiolite sequence and mainly occur as massive lava flows including basalts, basaltic andesites, andesites, dacites, and rhyolites. Dykes, ranging in composition from andesites to dacites and rhyolites intrude both intrusive and effusive ophiolitic rocks, as well as the calc-alkaline volcanics. Granitoids outcrop in the southwestern part of the SAM (Fig. 1) and mainly intrude ophiolites; they largely consist of granites and granodiorites, though diorites are locally found (Savu et al., 1996).

Ophiolites display an age of 167.8 ± 5 Ma (Nicolae et al., 1992), whereas the associated radiolarian cherts are Callovian to Oxfordian (Lupu et al., 1995). By contrast, the age of the calc-alkaline rocks is 155 Ma for granitoids (Pana, 1998) and 160 ± 5 Ma for volcanic rocks (Nicolae et al., 1992). Limestones intercalated in the upper part of the calc-alkaline volcanic sequence are Oxfordian to lowermost Tithonian.

Sampling and methods

The samples analysed in this paper represent an extensive geographical and stratigraphical coverage of the various calc-alkaline rock types cropping out in the C-T, Fenes, and Rimetea nappes (Fig. 1). Sampling focused mainly on volcanic products; a total of 55 samples were collected and analysed. Samples from the Fenes, and Rimetea nappes are regarded in this work as a single group, hereafter defined as the Trascau Mts. Nappes complex (T-M), because these nappes have the same geologic significance (Bortolotti et al., 2002).

Bulk rock major and trace elements analyses were determined on pressed powder pellets using an automated Philips PW1400 X-ray fluorescence (XRF) spectrometer. Matrix correction methods follow the methods proposed by Franzini et al. (1972).

Volatiles were determined as loss on ignition (LOI) at 1000 °C, while CO_2 contents were determined by volumetric technique (Jackson, 1958).

Rare Earth Elements (REE), Sc, Nb, Hf, Ta, Th, and U were determined by inductively coupled plasma-mass spectrometry (ICP-MS) using a VG Elemental Plasma Quad PQ2 Plus. Accuracy and detection limits were calculated by analysing a set of international standards.

Electron microprobe analyses were performed using a JEOL-JXA 8600 automated microanalyser. The operative conditions were: sample current of 10 nA and accelerating potential of 15 kV. Counting time was 100 s for peak and 20 s for background positions.

Both XRF and ICP-MS analyses were carried out at the Institute of Mineralogy of the University of Ferrara, while electron microprobe analyses were performed at the University of Florence.

Bulk-rock chemical compositions (Tables 1, 2), as well as microprobe analyses (Tables 3–5) are available on request in electronic form. See Website SMPM, contents of Vol 83/1, PDF file.

Petrography

Basalts and basaltic andesites from both C-T and T-M nappes display a porphyritic texture with porphyric index (PI) ranging from 30 to 80, with

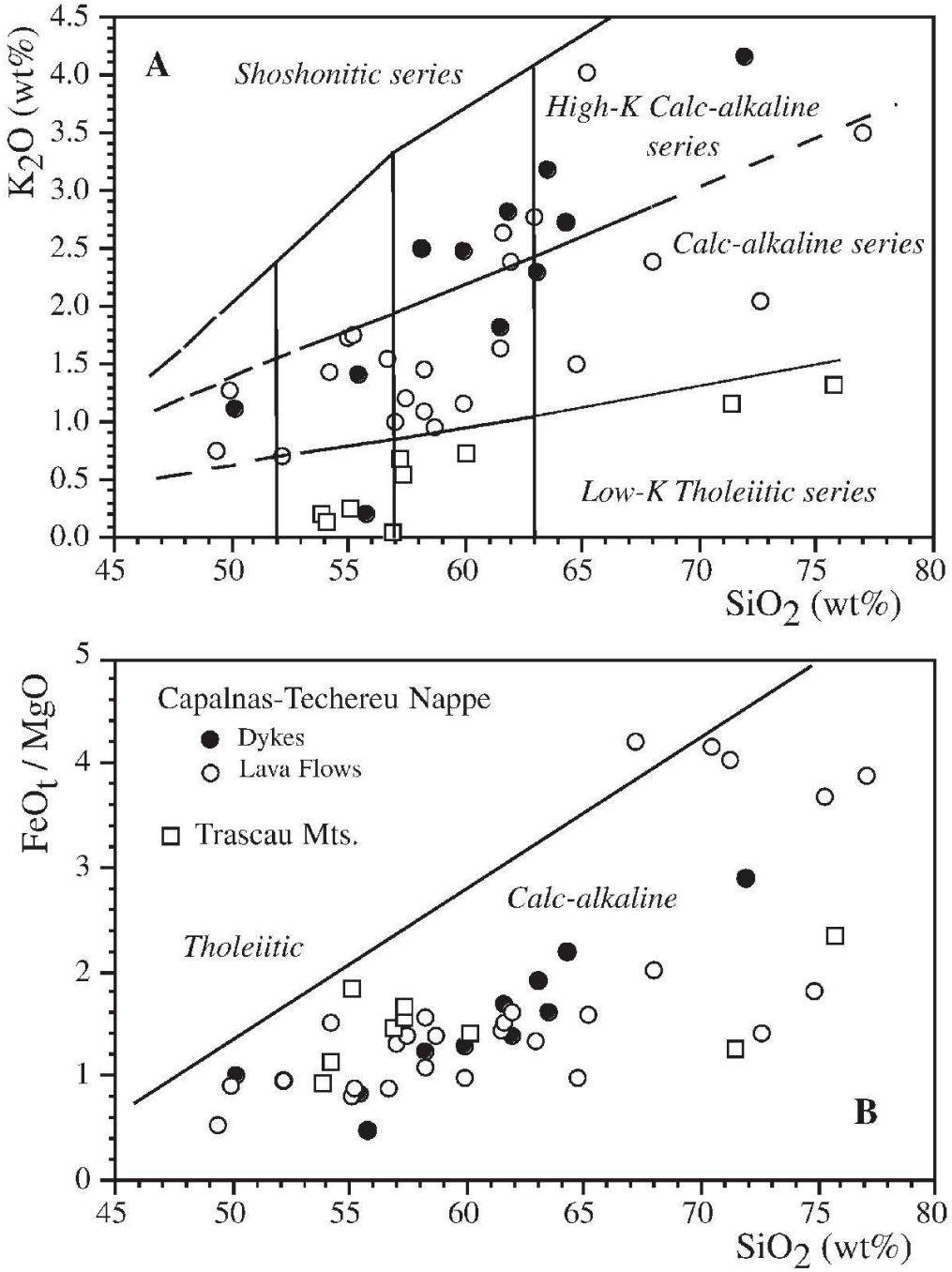

Fig. 2 (A) K_2O vs. SiO_2 diagram, modified after Peccerillo and Taylor (1976) and (B) SiO_2 vs. FeO_t/MgO diagram, modified after Miyashiro (1974), for the SAM Jurassic calc-alkaline volcanic volcanic suites. Trascau Mts. include Rimetea and Fenes Nappes.

phenocrysts of plagioclase, clinopyroxene and minor orthopyroxene. Olivine has not been observed, though in a few samples, pseudomorphs either of chlorite or calcite may be interpreted as former olivine. Phenocrysts of amphibole and quartz are rarely found in some of the basaltic andesites. They seem to be in equilibrium with their host lavas since no reaction coronae are observed. Groundmass textures range from vesiculated intergranular to hyalopilitic. Minerals in the groundmass consist of acicular laths of plagioclase and clinopyroxene, and more equant microphenocrysts of Fe-Ti oxides. In some samples few plagioclase phenocrysts contain melt inclusions.

All andesitic lavas have porphyritic to glomeroporphyritic textures (PI = 20–50). Phenocrysts assemblages include plagioclase, clinopyroxene, minor orthopyroxene, amphibole, and quartz showing resorbed grain boundaries, while Fe-Ti oxides usually occur as microphenocrysts and as inclusion in the other phenocryst phases. Groundmass textures range from hypocrystalline to hyalopilitic. Andesitic breccias are generally fine-grained and contain plagioclase, clinopyroxene, and andesitic fragments set in a glassy matrix.

Dacites are always aphyric with a hypocrystalline to glassy groundmass.

Rhyolites display a variety of textures, ranging from aphyric to moderately porphyritic and glomeroporphyritic (PI = 15–20). Phenocrysts include plagioclase, sanidine, quartz with resorbed grain boundaries, amphibole, biotite, and Fe-Ti oxides. The groundmass is typically hyalopilitic, and in some samples perlitic textures are observed.

Dykes display textures similar to those observed in the corresponding rock types from massive lava flows. Some dykes are characterised by porphyritic cores and aphyric borders.

The granitic rocks exhibit a coarse-grained hypidiomorphic texture, containing idiomorphic plagioclase, sub-idiomorphic amphibole, biotite and orthoclase, and anhedral quartz. Accessory phases include sphene, apatite, and zircon.

Textural associations and phenocryst assemblages described above suggest the following crystallisation sequence: olivine, plagioclase, Fe-Ti oxides, clinopyroxene, and orthopyroxene for basalts and basaltic andesites, followed by amphibole, biotite, and quartz in the andesitic-dacitic-rhyolitic series.

Some of the studied rocks have been subject to various degrees of alteration, possibly occurred under very low grade metamorphic conditions. When present, alteration is usually moderate in the C-T Nappe samples and moderate to severe in the T-M rocks. Alteration products include albite, replacing plagioclase; sericite, usually pseudomorphic after feldspar; calcite, replacing plagioclase and olivine; and chlorite replacing mafic phases. Chlorite also developed extensively in the groundmass of all studied rocks types.

Whole-rock chemistry

K_2O contents of SAM lavas are plotted vs. SiO_2 in the diagram of Peccerillo and Taylor (1976) shown in Fig. 2a. In this diagram a general compositional difference between volcanic rocks from the T-M and C-T nappes is observed. Most of the volcanic rocks from the T-M nappes exhibit an apparent low-K tholeiitic affinity, ranging in composition from low-K basaltic andesite to andesite and rhyolite, although medium-K andesites are also present. By contrast, most of the volcanic rocks from the C-T Nappe belong to a calc-alkaline series, with compositions from calc-alkaline basalts to rhyolites via basaltic andesites, andesites, and dacites. In addition, some high-K calc-alkaline andesites occur. Dykes from the C-T Nappe show compositions ranging from calc-alkaline basalts, basaltic andesites, and andesites to high-K calc-alkaline andesites and dacites. Among dykes the high-K calc-alkaline types prevail. However, the apparent low-K tholeiitic affinity displayed by most of the T-M samples is in contrast with their general mineralogical and geochemical features (as presented below). In fact, T-M rocks are characterised by a high degree of alteration, which has resulted in a general loss of alkalis, especially K_2O. Consequently, while the classification scheme of Fig. 2a can be accepted for the C-T nappe rocks, it cannot be taken at face value for the T-M samples, for which a calc-alkaline affinity can also be postulated, on the basis of Miyashiro's classification diagram shown in Fig. 2b (Miyashiro, 1974).

The common trends displayed by C-T and T-M rocks on the variation diagrams (Fig. 3) suggest that their magmatic evolutions were characterised by similar processes and parental magma compositions.

The elemental variation (Fig. 3) present a characteristic calc-alkaline trend of decreasing FeO_t, TiO_2, MgO, Cr, and V with increasing SiO_2. Al_2O_3, CaO, and P_2O_5 show an increasing pattern towards the more evolved rocks (dacites and rhyolites). The immobile incompatible high field strength elements (HFSE), such as Zr, Y, and Ce, show clear positive correlation trends with SiO_2. Similar trends are displayed by large ion lithophile elements (Ba and Rb). Despite considerable alteration of some samples, the covariation of Rb throughout the suite is fairly strong, sug-

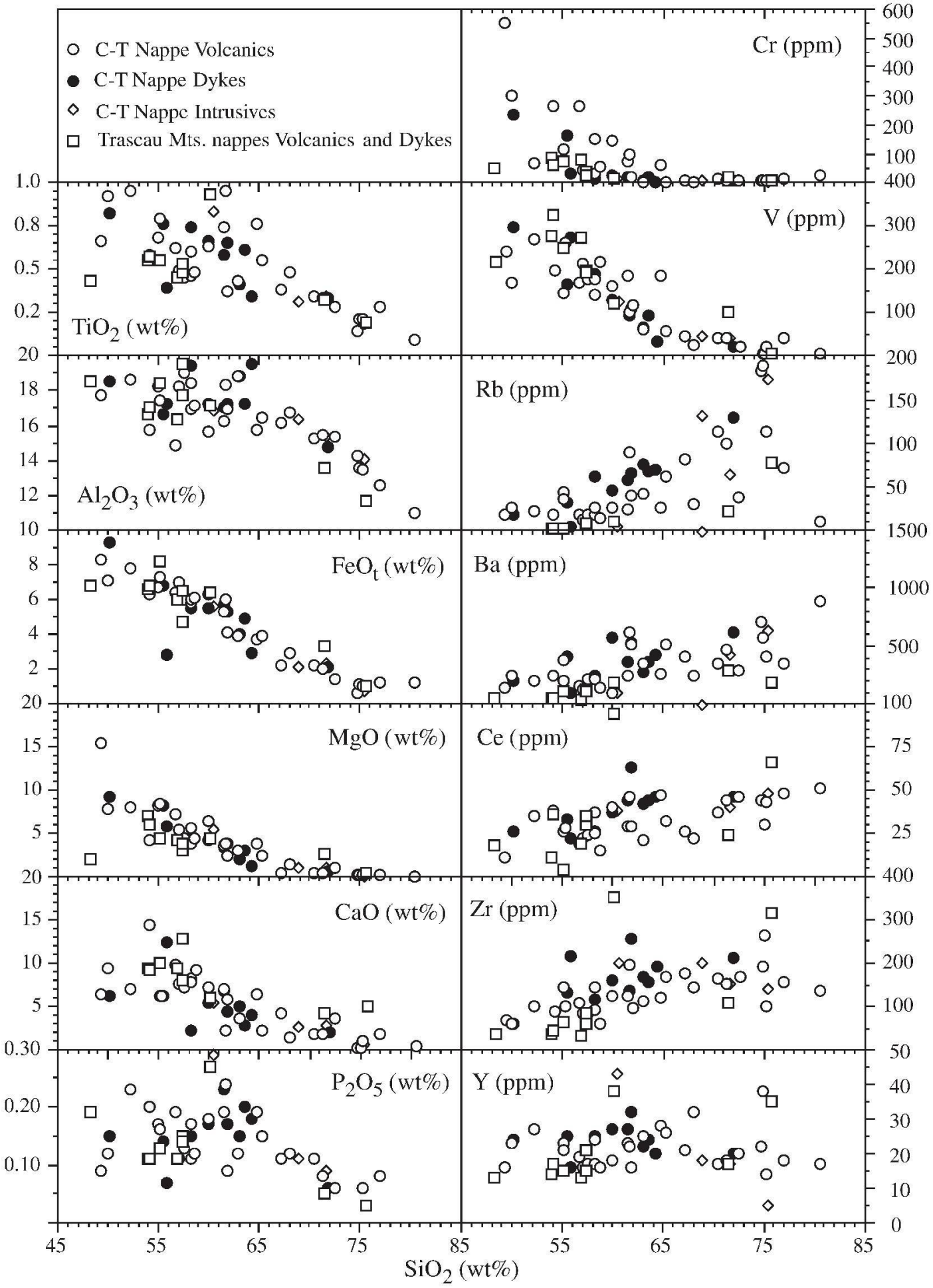

Fig. 3 Selected major and trace element vs. SiO_2 variation diagrams for the SAM Jurassic calc-alkaline rocks. C-T — Capalnas-Techereu.

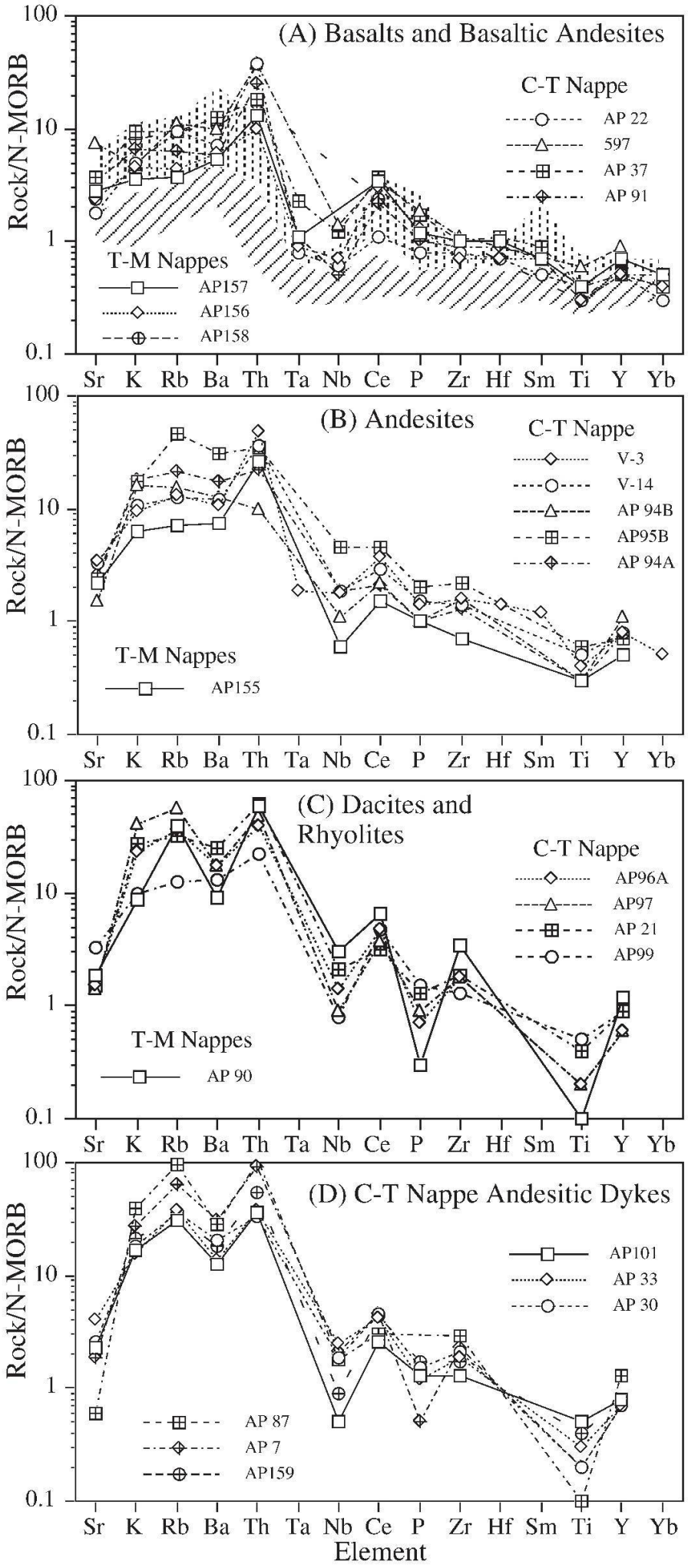

Fig. 4 Rock/N-MORB incompatible elements diagrams for selected Jurassic volcanic and subvolcanic calc-alkaline rocks from SAM. Normalisation values and compositions of typical island arc basalts are from Pearce (1983). Hatched field: calc-alkaline basalts; dashed field: tholeiitic basalts.

gesting that loss of K was not coupled with a systematic loss of Rb. Intrusive rocks define trends similar to those of the volcanic rock (Fig. 3).

Basalts and basaltic andesites from both C-T and T-M nappes exhibit trends which are very similar to those of oceanic calc-alkaline basalts (Fig. 4a) with marked enrichment in Sr, K, Rb, Ba, Th, and Ce, and with depletion in Nb, Ti (and Ta). The magnitude of both positive and negative anomalies become stronger in the more evolved lavas (andesites, dacites and rhyolites), in which a significant P negative anomaly and Rb positive anomaly are observed (Figs. 4b, c). Furthermore, these rocks show decreasing abundances of HFSE, such as P, Zr, Ti, and Y, with increasing SiO_2. Andesitic dykes display incompatible element compositions very similar to those observed for volcanic rocks (Fig. 4d).

Chondrite-normalized rare earth elements (REE) patterns (Fig. 5) display a marked light REE (LREE) enrichment with respect to heavy REE (HREE), with $(La/Yb)_N$ ratios ranging from 2.3 to 6.3. These LREE enrichments are consistent with the calc-alkaline affinity of the studied rocks. Enrichment factors for LREE (e.g. La) vary from 17 times chondrite in basalts to 60 times chondrite in basaltic andesites and 80 times chondrite in andesites. The convex-upward mid-REE variations suggest that amphibole fractionation occurred. No systematic differences in the magnitude of HREE depletion with increasing SiO_2 contents are observed. In addition, very slightly negative Eu anomalies are observed in some samples.

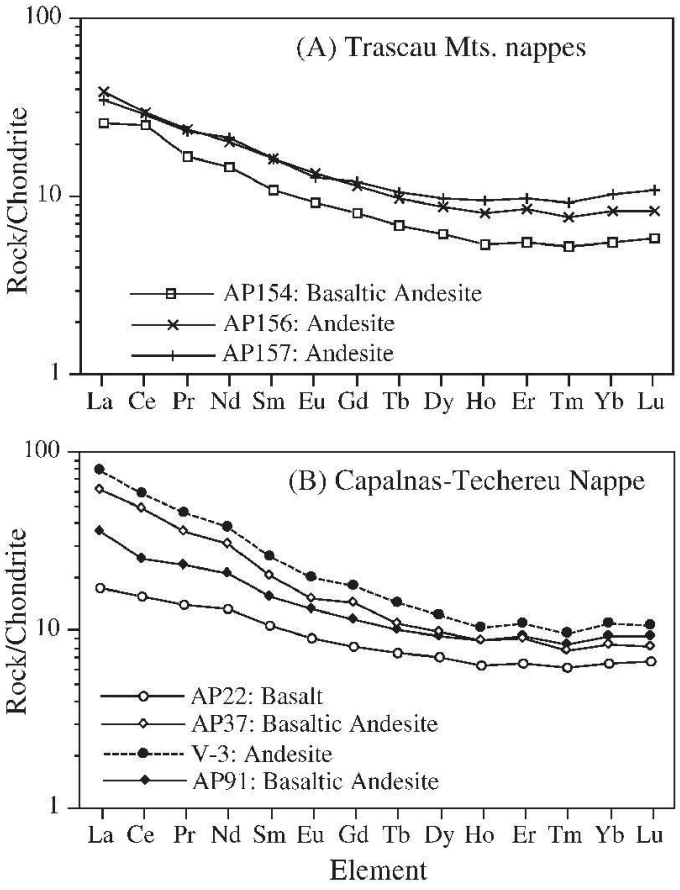

Fig. 5 Chondrite-normalized REE patterns for selected volcanic and subvolcanic Jurassic calc-alkaline rocks from SAM. Normalisation values are from Sun and McDonough (1989).

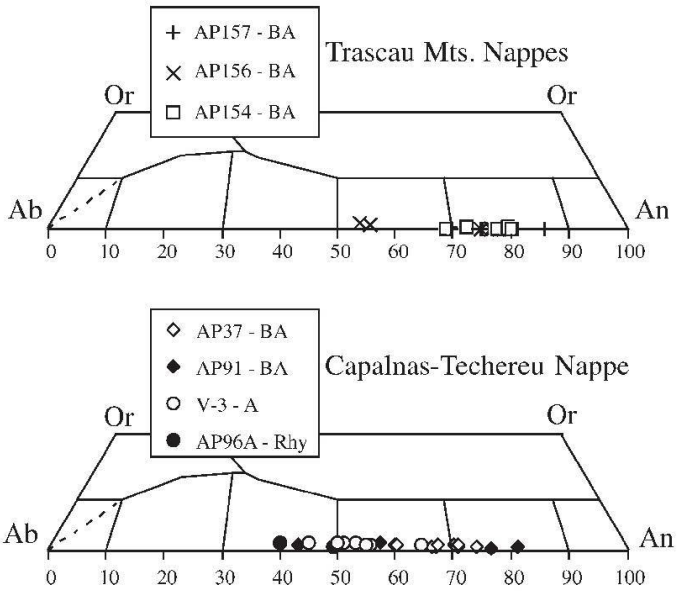

Fig. 6 Compositions of plagioclase from the South Apuseni Mountains ophiolites. BA—basaltic andesite; A—andesite; Rhy—rhyolite.

Mineral chemistry

Plagioclase

Representative compositions of plagioclase phenocrysts and groundmass microlites are illustrated in Fig. 6.

Compositions of phenocryst cores in basaltic andesites from the T-M nappes are in the range An_{80}–An_{68}, while compositions of plagioclase groundmass microlites are characterised by lower An contents (An_{50}–An_{53}). Generally, phenocrysts display An decrease from core to rim. Groundmass microlites and rims of phenocrysts from basaltic andesites have compositions that are either normally or reversely zoned in relation to core composition, with compositional differences between cores and rims or microlites that may reach 15 mol% An. By contrast, groundmass microlites and phenocryst rims from andesites and rhyolites have compositions that are reversely zoned relative to core compositions. The compositional differences between cores and rims may reach 9 mol% An.

Some samples from both C-T and T-M nappes contain a small percentage of plagioclase grains that are finely sieved owing to a network of inter-

connected glass inclusions, usually concentrated in the phenocryst cores.

The observed zoning characteristics together with the presence of sieve-textured crystals have been interpreted by Tsuchiyama (1985) as the result of magma mixing phenomena, and by Nelson and Montana (1992) as resulting from rapid adiabatic decompression during magma ascent. Moreover, some of the sieve-textured plagioclases may represent xenocrysts derived from disaggregation of previously formed rocks. A distinction of the relative importance of these processes is difficult because they produce very similar results.

Pyroxene

Representative analyses of pyroxenes from SAM lavas are illustrated in Fig. 7. Both ortho- and clinopyroxene are present in the T-M nappes basaltic andesites, where orthopyroxene is usually less abundant than clinopyroxene. By contrast, orthopyroxene is not present in the C-T Nappe lavas. Clinopyroxene compositions lie predominantly in the diopsidic and augitic fields, slightly extending to magnesium-rich augite, while the subcalcic compositions (Fig. 7) characteristically occur as groundmass microlites. Orthopyroxene compositions lie in the enstatite field.

Most clinopyroxenes in basaltic andesites and andesites show reverse zoning, as exemplified by the variations of the Mg-number [Mg#: 100 Mg/(Mg + Fe^{2+})] that range from 73.4 to 75.4, and from 73.6 to 88.4 in cores and rims, respectively. There is no systematic difference in Al-, Na- or Ti-contents between cores and rims in any of the rock types.

The FeO_t/MgO ratios in clinopyroxenes from T-M lavas exceed those observed in clinopyroxenes from the C-T Nappe. In basaltic andesites from both localities the Mg# values of clinopyroxene phenocrysts roughly decrease with increasing FeO_t/MgO ratios, while in andesites they are greater than in the less evolved lavas. Mg# values in clinopyroxene are also greater than those observed in the coexisting orthopyroxene. Decreasing Mg# values in the order clinopyroxene > orthopyroxene > amphibole associations are consistent with early crystallization of clinopyroxene, followed by orthopyroxene and amphibole.

Clinopyroxenes show compositions (Fig. 8a) that are typical of orogenic-type basalts (Leterrier et al., 1982) and predominantly lie in the calc-alkaline field (Fig. 8b).

Amphibole

Amphiboles in both the T-M and C-T calc-alkaline series are found in the more evolved lavas (i.e. andesites, dacites, and rhyolites), and are usually altered to tremolite-actinolite. Fresh amphiboles are found only in rocks belonging to the C-T Nappe, where they usually occur as phenocrysts and microphenocrysts, and can be classified as Mg-hornblende (Leake, 1978). Compositional variation for the analysed amphibole phenocrysts shows a smooth correlation with increasing differ-

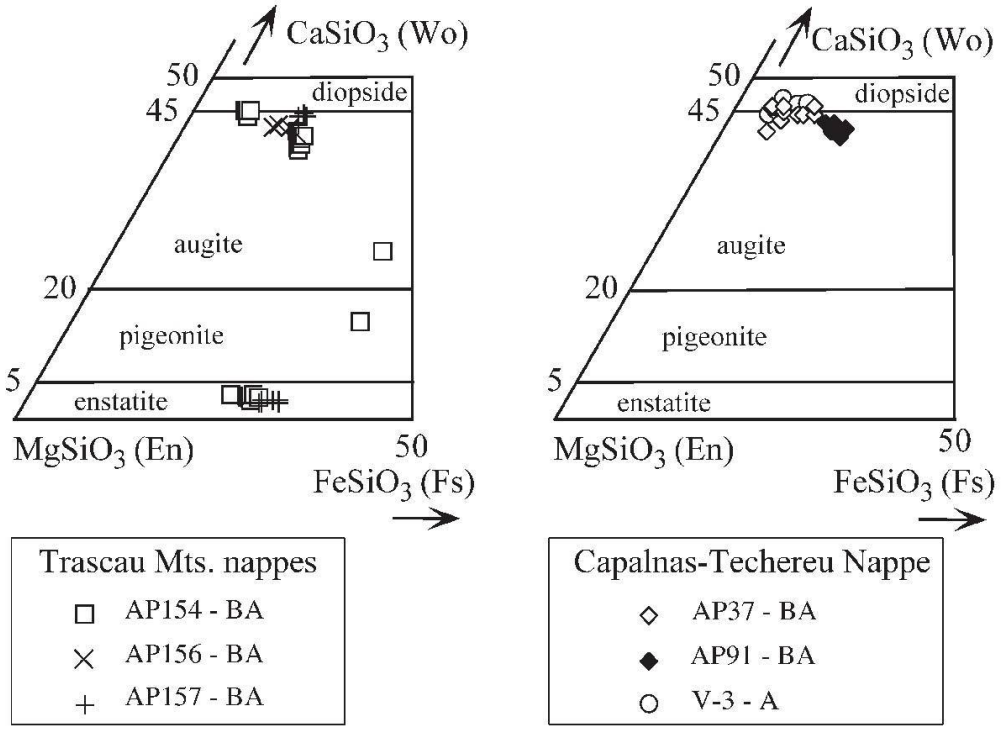

Fig. 7 Plots of pyroxene compositions expressed in terms of Enstatite-Ferrosilite-Wollastonite for SAM Jurassic calc-alkaline rocks. Abbreviations as in Fig. 6.

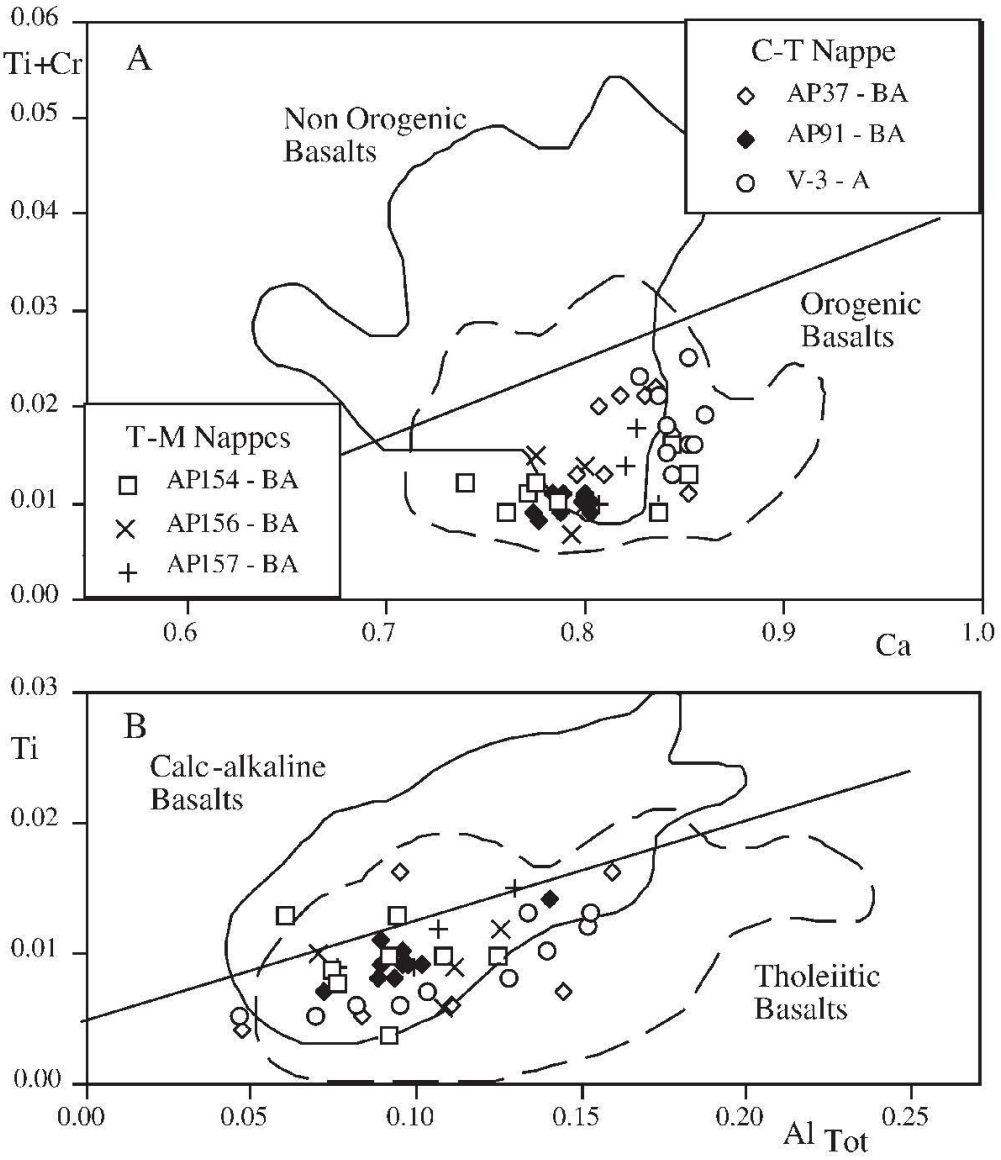

Fig. 8 Discrimination diagram for clinopyroxenes from SAM Jurassic calc-alkaline basaltic rocks, after Leterrier et al. (1982). (A) discrimination between non-orogenic and orogenic basalts; (B) discrimination between calc-alkaline and tholeiitic basalts. Abbreviations: T-M—Trascau Mts., other abbreviations as in Fig. 6.

entiation. This correlation is exemplified by the variation in Mg# and (Na + K) contents which are, respectively, 81.7–70.3 and 0.406–0.502 in andesite, 78.8–67.5 and 0.380–0.682 in rhyolite. Similarly, (Na + K) and Mg increase from core to rim in amphibole phenocrysts from andesitic lavas.

Discussion

Equilibrium phenocryst assemblages

The petrological evolution of the SAM calc-alkaline series can be traced by observing the relationships between mineral phases and whole-rock composition, by examining if the mineral-whole-rock compositions are in equilibrium, and whether compositional variations within phenocrysts and compositional variations between phenocrysts and groundmass microlites are indicative of fractional crystallization or magma mixing phenomena.

Assuming that the whole-rock composition is representative of the liquid present within the magma chamber, if the system remained closed, the phenocryst core compositions would be in equilibrium with the bulk rock compositions. If whole-rock and phenocryst cores were in equilibrium, then plots of CaO/Na_2O in plagioclase vs. whole-rock CaO/Na_2O (Fig. 9) would be consistent with experimentally determined distribution coefficients.

Experimental work by Sisson and Grove (1993) on basalts and basaltic andesites shows that K_D^{Ca-Na} values for plagioclase-melt equilibrium depend on water contents. K_D^{Ca-Na} values increase from about 1 for anhydrous conditions to 5.5 for water-saturated magmas at 2 kbar, and are relatively independent of pressure. Experiments also indicate that differentiation processes, at con-

stant water content, do not significantly affect the K_D value for plagioclase, consequently, these values can also be applied to fairly evolved magmas (Sisson and Grove, 1993).

The plagioclase-whole-rock CaO/Na_2O ratios for the studied samples display slightly scattered plots (Fig. 9). The studied samples contain plagioclase in equilibrium or near-equilibrium with the bulk composition at any given K_D value (i.e. at any given water content), suggesting that the whole rock composition may reasonably represent the magma composition for most samples. This conclusion is further supported by the lack of petrographic evidence of cumulus processes. An exception is represented by sample AP91, in which considerable scatter of plagioclase CaO/Na_2O ratios is observed. This rock contains plagioclases which are both too primitive and too evolved to have crystallised from a liquid of the bulk composition for any of the predicted K_D values. Possible explanations for these compositional variations include: (1) plagioclase represents different crystal populations inherited from different liquid batches during magma mixing; (2) early formed plagioclase crystals have not reacted with the liquid from which they formed, and thus represent phases that are not in equilibrium with the host magma; (3) non-equilibrium plagioclases are xenocrysts.

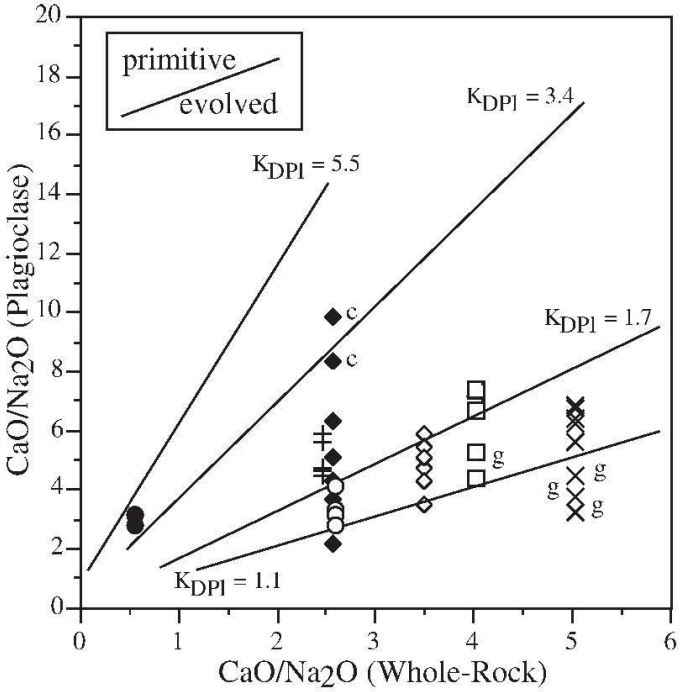

Fig. 9 Plots of CaO/Na_2O ratios of plagioclase analyses and whole-rock compositions from SAM Jurassic calc-alkaline rocks. According to Sisson and Grove (1993), K_D values are: 1.1 for anhydrous melts; 1.7 for H_2O = 2%; 3.4 for H_2O = 4%; 5.5 for water-saturated melts. c—crystal core; g—groundmass microlite. Symbols as in Fig. 6.

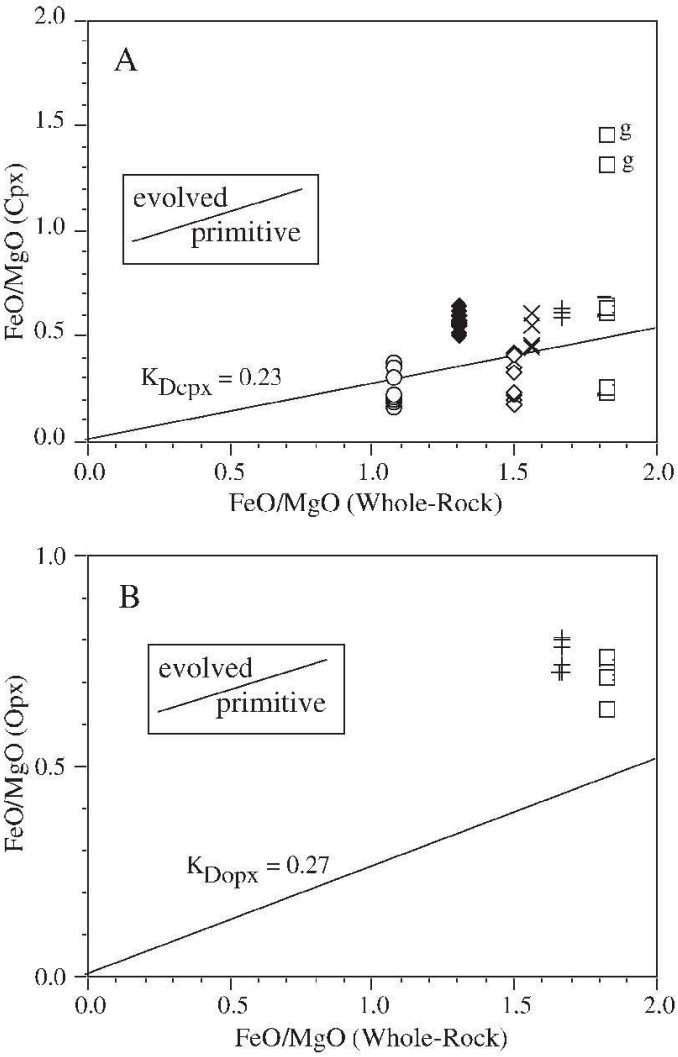

Fig. 10 Plots of FeO/MgO ratios of clinopyroxene (A) and orthopyroxene (B) analyses and whole-rock compositions from SAM Jurassic calc-alkaline rocks. Theoretical equilibrium K_D values are from Grove and Bryan (1983); Kay and Kay (1985); Sisson and Grove (1993). g—groundmass microlite. Symbols as in Fig. 6.

Groundmass microlites in samples AP154 and AP156 display compositions that are too evolved to have crystallised from a liquid corresponding to the whole-rock composition, suggesting that groundmass microlites possibly crystallised from a residual liquid portion that is more evolved than the bulk composition. This conclusion is in accordance with the high modal amount of phenocrysts in these rocks.

In addition, Fig. 9 shows that plagioclase from more evolved rocks plots across K_D lines corresponding to increasing water contents.

In summary, plagioclase from most of the studied rocks grew under near-equilibrium conditions, suggesting that fractional crystallization in closed systems was the main fractionation process.

Similar conclusions apply to pyroxene phenocrysts. If whole-rock and phenocryst cores are in equilibrium, then the diagrams of FeO/MgO in

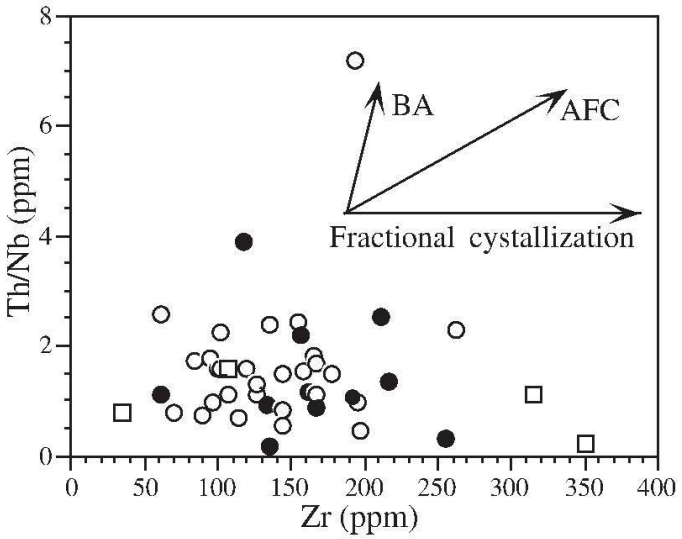

Fig. 11 Zr vs. Th/Nb plot for volcanic and sub-volcanic rocks from SAM Jurassic calc-alkaline rocks. Schematic trends reflecting increasing fractional crystallization (FC), assimilation-fractional crystallization (AFC), and bulk assimilation (BA) are also reported. Symbols as in Fig. 2.

pyroxenes vs. whole-rock FeO/MgO (Fig. 10) should be consistent with experimentally determined distribution coefficients (Grove and Bryan,1983; Kay and Kay, 1985; Sisson and Grove, 1993).

In fact, most of the clinopyroxene analyses displayed in Fig. 10a lie very close to the equilibrium K_D line. This suggests that most of the pyroxene cores coexisted in equilibrium with the whole-rock composition. Similarly to what has been observed for plagioclase above, clinopyroxene

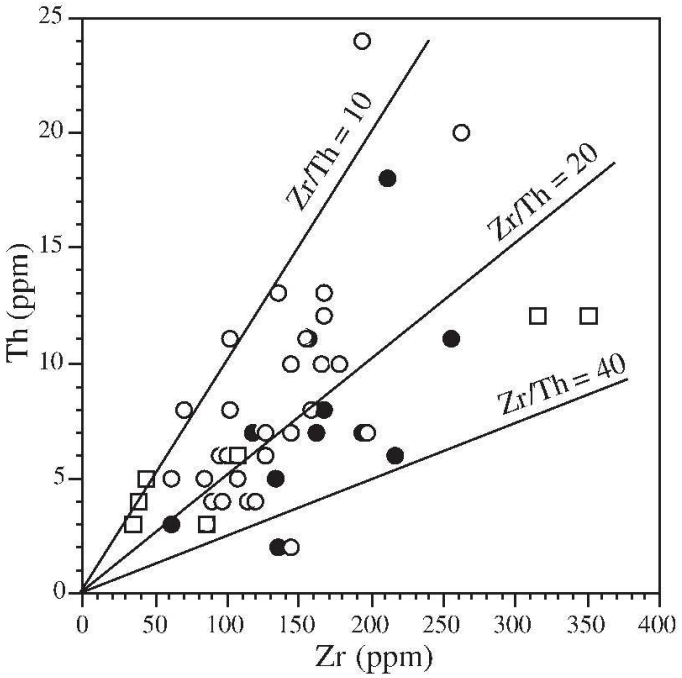

Fig. 12 Zr vs. Th plot for volcanic and sub-volcanic rocks from SAM Jurassic calc-alkaline rocks. Symbols as in Fig. 2.

groundmass microlites from sample AP154 seem to be in equilibrium with a residual liquid which is more evolved than the bulk composition.

Orthopyroxene analyses from samples AP154 and AP157 (Fig. 10b) seem to be too evolved for the whole-rock liquid composition. Variations in Mg# in orthopyroxenes from samples AP154 (73.8–70.2) and AP157 (71.4–69.0) indicate no significant compositional zoning. These facts can be explained by later crystallisation of orthopyroxene from a more evolved liquid just prior to eruption; this interpretation is consistent with textural evidence.

As observed for plagioclase, the compositions of pyroxenes are consistent with fractional crystallization processes, as also suggested by the good correlation between FeO/MgO ratios of pyroxene phenocrysts and the whole-rock SiO_2 contents.

Geothermometry and geobarometry

Magmatic temperatures have been calculated on basaltic andesites using a variety of two-pyroxene and one-pyroxene geothermometers (Wood and Banno, 1973; Bertrand and Mercier, 1985–86; Brey and Kohler, 1990) on equilibrium pyroxenes (Fig. 9). The best results were obtained from the two-pyroxene method proposed by Brey and Kohler (1990). For pyroxene pair compositions from basaltic andesite AP154, estimated temperatures are 1216 °C (analytical uncertainty ± 15 °C) and 1147 ± 4 °C for cores and rims, respectively. Calculations made on pyroxenes from andesite AP157 give estimated temperatures of 1140 ± 15 °C for phenocryst cores, and 1137 ± 15 °C for rim compositions.

Magmatic temperatures for rhyolites have been estimated using the geothermometer proposed by Blundy and Holland (1990), which is based on the amphibole-plagioclase equilibrium, mostly on phenocryst core compositions. Phenocryst rim analyses were also used for comparison with the cores, but no systematic differences were observed. Estimated temperatures are 860 ± 10 °C.

The pressure of formation of phenocryst cores has been calculated for andesites and rhyolites from the C-T Nappe using the geobarometer proposed by Hammarstrom and Zen (1986), which is based on the Al-content of amphibole for a temperature range of 700–900 °C. The estimated pressures for hornblende are in the range of 1.8–2.3 kbar for both andesite and rhyolite.

Although the previously reported data do not refer to a single stratigraphical unit, the observed variations in temperature along the fractionation trend are consistent with a progressive magmatic

cooling in closed systems, at pressures included between 1.8–2.3 kbar, from pre-eruptive temperatures of 1216 °C for the less evolved rocks down to 860 °C for the more evolved rocks.

Petrogenesis and tectono-magmatic setting

Volcanic rocks from both T-M and C-T calc-alkaline series display good correlations with silica in the variation diagrams of Fig. 3, suggesting that crystal fractionation was the most important process during the petrogenetic evolution of these magmatic series. The elemental variations (Fig. 3) are consistent with fractionation of the observed phenocryst minerals (i.e., plagioclase, clinopyroxene, orthopyroxene, amphibole, and titanomagnetite). In addition, the limited scatter displayed by many elements accounts for a magmatic evolution from parental magmas bearing very similar compositions.

Fractionation of plagioclase in the most primitive liquids can readily explain the decrease of Sr/Y with increasing SiO_2, while fractionation of amphibole was important during the evolution at the intermediate-late magmatic stages, as suggested by the increase of the La/Yb ratios, as well as the chondrite-normalized REE patterns with a concave-upward shape towards the more evolved rocks (Romick et al., 1992).

Possible contributions from the lower crust to magma compositions (e.g. assimilation-fractional crystallization (AFC) process (DePaolo, 1981), as well as magma mixing phenomena are investigated using the Th/Nb elemental ratios plotted vs. Zr (Fig. 11). In this diagram LILE/HFSE ratios, which should not be significantly affected by fractional crystallisation, are plotted against an incompatible trace element whose abundance increases as fractionation increases. Such a diagram allows the distinction between magmatic evolutions controlled by simple fractional crystallisation in closed systems, that will produce an almost horizontal trend with increasing fractionation, and those influenced by additional processes. SAM rocks define trends characterised by fairly constant Th/Nb elemental ratios (Fig. 11), implying that fractional crystallization is by far the most effective process during magmatic differentiation. However, a few samples exhibit higher Th/Nb ratios than other rocks. These represent dykes crosscutting intermediate, calc-alkaline volcanics; thus the simplest explanation for their high Th/Nb ratios is assimilation of their host rocks.

Similar conclusions can be reached by observing the generally high Zr/Th ratios displayed by SAM calc-alkaline rocks (Fig. 12). Actually, HFSE/LFSE ratios are greater in intraoceanic-arc lavas than in continental-arc lavas, because LFSE are expected to be partitioned more efficiently than HFSE into the crustal portions, which are more susceptible to assimilation (Hildreth and Moorbath, 1988).

In addition, Nb/Th ratios (0.60–0.96) are quite uniform and independent of SiO_2 variations, suggesting no influence of crustal assimilation during differentiation.

Hf/Ta (6.1–11.9) ratios are generally low and are similar to those of Quaternary volcanics from the southern part of the Southern Volcanic Zone of the Andes, which is interpreted as essentially uncontaminated by continental crust (Hildreth and Moorbath, 1988).

Several studies have demonstrated that HREE and HFSE contents in many arc lavas are lower than typical MORB values (e.g., Pearce, 1983). This suggests that many island arc basalts originate from sources depleted in incompatible elements as compared to basalts derived from variable degrees of melting of a normal MORB source. Hence a melt extraction prior to arc magma generation is required to explain the depletion of incompatible elements observed in arc lavas. Unfortunately, a direct observation of the nature of the sub-arc mantle cannot be made in the SAM. The depletion in HREE and HFSE contents observed in SAM calc-alkaline lavas is nonetheless consistent with the above hypothesis.

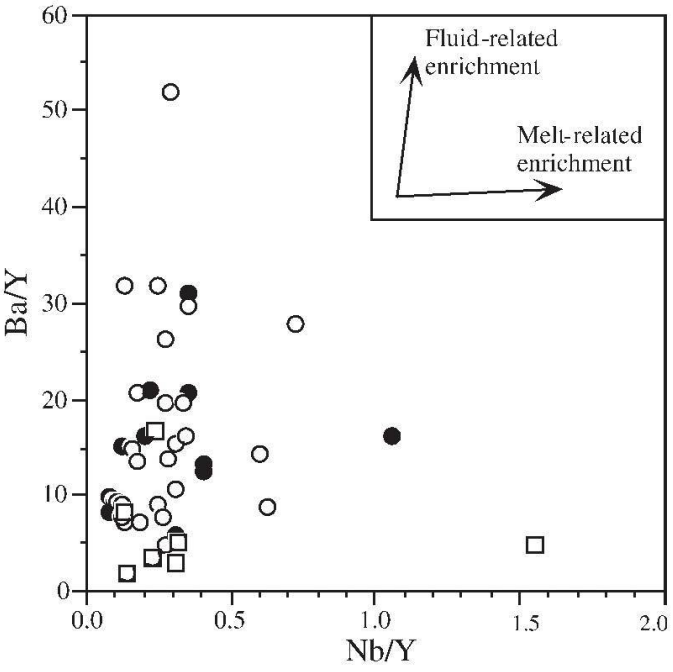

Fig. 13 Nb/Y vs. Ba/Y plot for volcanic and sub-volcanic rocks from SAM Jurassic calc-alkaline rocks. Schematic trends related to increasing hydrous metasomatism and slab melt enrichment are from Kapezhinskas et al. (1997). Symbols as in Fig. 2.

According to the general model currently accepted for the genesis of arc magmas, the LREE and LILE enrichments observed in SAM calc-alkaline lavas can be referred to a chemical contribution from subduction-derived components. Figure 13 shows an attempt to discriminate between fluid-related and melt-related enrichments (Hole et al., 1984; Defant and Drummond, 1990) by plotting Ba/Y ratios versus Nb/Y ratios for analysed samples. HFSEs, such as Nb and Y, have a very low potential to partition into hydrous fluids. On the other hand, melt-derived enrichment processes will drive compositions toward high Nb/Y ratios since slab melts are depleted in Y due to the retention of this element in the residual garnet in the slab under amphibolite facies conditions (Defant and Drummond, 1990). By contrast, LILEs such as Ba have high potential to partition into fluids, so that fluid-derived enrichment will drive compositions toward high Ba/Y ratios. Fig. 13 shows that the majority of lavas from both C-T and T-M nappes follow the enrichment trend related to slab-derived hydrous fluids.

In summary, data presented in this paper indicate that SAM Jurassic calc-alkaline rocks originated by fractional crystallization in a closed system from primary melts derived, in turn, from a depleted mantle source enriched in LILE and LREE by slab-derived hydrous fluids. Various incompatible trace element ratios indicate that primary melts derived from very similar source compositions, and that possible contributions of the lower crust to the magma compositions (e.g. by an AFC process; DePaolo, 1981) or mixing between different magma types are generally very subordinate or absent. The overall chemical and petrological characteristics suggest that these calc-alkaline rocks originated in an intra-oceanic island arc setting.

Burchfiel (1980) and Zacher and Lupu (1998), suggested that the pre-Miocene position of the SAM was in the northern prolongation of the Dinaride-Hellenide Vardar Zone, and that they were displaced to their present-day location by a dextral transpression along the South Transylvanian fault system. Accordingly, Bortolotti et al (2002) documented close similarities between SAM and Vardar Zone ophiolites.

According to this reconstruction, the SAM calc-alkaline series record a Late Jurassic intra-oceanic subduction developed in the northernmost sector of the Vardar oceanic basin, in a convergence tectonic setting related to the closure of the Vardar ocean. Ophiolites underlying the calc-alkaline series were generated at a mid-ocean spreading ridge and do not display any intra-oceanic subduction feature (Saccani et al., 2001; Bortolotti et al., 2002). This fact, together with data presented in this paper indicates that, in contrast to previous reports (Radulescu and Sandulescu, 1973; Cioflica and Nicolae, 1981), no genetic relation between island arc activity and ophiolites exists.

Conclusions

1) The Jurassic SAM calc-alkaline series surfacing in both C-T and T-M nappes are closely associated to Jurassic ophiolites, and mainly consist of volcanic rocks covering a wide range in composition (from basalt to rhyolite). Subordinate granitic bodies, intruding ophiolites, as well as dykes, intruding both ophiolitic and calc-alkaline sequences, also occur. Dykes range from basaltic andesites to dacites and rhyolites.

2) The SAM calc-alkaline series display major and trace element abundances consistent with fractional crystallization in closed systems as the dominant evolutionary process. Phenocryst assemblages display equilibrium or near-equilibrium relationships with the whole-rock compositions, further supporting this conclusion. Possible contributions of the lower crust to the magma compositions or fractionation from different primary magmas, in turn reflecting variable source compositions, are considered quite subordinate.

3) Pressures of formation, estimated from phenocryst assemblages, are about 1.8–2.3 kbar, while temperatures range from 1216 °C in basaltic rocks to 860 °C in rhyolites.

4) LILE/HFSE and HFSE/LFSE ratios observed for SAM calc-alkaline lavas are very similar to those observed in modern intra-oceanic arcs. Parental magmas probably originated from partial melting of a depleted mantle source further enriched in LILEs by fluid phases derived from the dehydration of the subducting oceanic plate; nonetheless, the intensity of enrichment in fluids is variable. No contribution from subduction-derived melts is observed.

The results outlined above suggest that the Late Jurassic calc-alkaline rocks from the South Apuseni Mountains (SAM) probably originated in an island-arc setting. The spatial and temporal relationships between the calc-alkaline and ophiolitic (Saccani et al., 2001) sequences suggest that the island arc magmatic activity developed over an intra-oceanic sub-arc crust now represented by the ophiolitic rocks. Consequently, in contrast to previous interpretations (Radulescu and Sandulescu, 1973; Cioflica and Nicolae, 1981), no genetic relationship between the calc-alkaline series and ophiolites is postulated.

According to regional recontructions (Burchfiel, 1980; Zacher and Lupu, 1998), the pre-Miocene position of the SAM was in the northern prolongation of the Vardar Zone of the Dinaride belt. Thus, we postulate that the SAM calc-alkaline suites testify to a Late Jurassic intra-oceanic subduction developed during the closure of the northernmost sector of the Vardar oceanic basin.

Data presented in this paper may provide significant constraints for the further geodynamic reconstruction of the northernmost border of the Vardar ocean and its related continental margins.

Acknowledgements

We gratefully acknowledge L. Beccaluva for his helpful comment on the early version of this paper, V. Bortolotti, M. Marroni, L. Pandolfi, and G. Principi for field assistance, as well as R. Tassinari and F. Olmi for analytical assistance. We also thank V. Morra and an anonymous referee for very constructive journal reviews. This work was supported by MURST-COFIN grants and by the Geological Institute of Romania.

References

Bertrand, P. and Mercier, J.-C.C. (1985): The mutual solubility of coexisting ortho- and clino-pyroxene: toward an absolute gothermometer for the natural system? *Earth Planet. Sci. Lett.* **76**, 109–122.

Blundy, J.D. and Holland, T.J.B. (1990): Calcic amphibole equilibria and a new amphibole-plagioclase geothermeter. *Contrib. Mineral. Petrol.* **104**, 208–224.

Bortolotti, V., Nicolae, I., Marroni, M., Pandolfi, L., Principi, G. and Saccani, E. (2002): Geological and petrological evidences for Jurassic association of ophiolite and Island arc volcanics in the South Apuseni Mountains (Romanian Carpathians). *Int. Geology Rev.* **44(10)**, 938–955.

Brey, G.P. and Kohler, T. (1990): Geothermobarometry in four-phase lherzolites II. New thermobarometers, and practical assessment of existing thermobarometers. *J. Petrol.* **31**, 1353–1378.

Burchfiel, B.C. (1980): Eastern european alpine system and the Carpathian orocline as an example of collision tectonics. *Tectonophysics* **63**, 31–61.

Cioflica, G. and Nicolae, I. (1981): The origin, evolution and tectonic setting of the Alpine ophiolites from the South Apuseni Mountains. *Rev. Roum. Géol. Géophys. Géogr.* **25**, 19–29.

Dallmeyer, R.D., Pana, D.I., Neubauer, F. and Erdmer, P. (1999): Tectonothermal evolution of the Apuseni Mountains, Romania: resolution of Variscan versus Alpine events with $^{40}Ar/^{39}Ar$ ages. *J. Geol.* **107**, 329–352.

Dal Piaz, G.V., Martin, S., Villa , I.M. and Gosso, G. (1995): Late Jurassic blueschist facies pebbles from the Western Carpathians orogenic wedge and paleostructural implications for Western Tethys evolution. *Tectonics* **14**, 874–885.

Defant, M.J. and Drummond, M.S. (1990): Derivation of some modern arc magmas by melting of young subducted lithosphere. *Nature* **347**, 662–665.

DePaolo, D.J. (1981): Trace element and isotopic effects of combined wallrock assimilation and fractional crystallization. *Earth Planet. Sci. Lett.* **53**, 189–202.

Franzini, M., Leoni, L. and Saitta, M. (1972): A simple method to valutate the matrix effect in X-ray fluorescence analysis. *X-Ray Spectrometry* **1**, 151–154.

Grove, T.L. and Bryan, W.B. (1983): Fractionation of pyroxene-phyric MORB at low pressure: An experimental study. *Contrib. Minaral. Petrol.* **84**, 293–309.

Hammarstrom, J.M. and Zen, E-an (1986): Aluminium in hornblende: an empirical geobarometer. *Am. Mineral.* **71**, 1297–1313.

Hildreth, W. and Moorbath, S. (1988): Crustal contribution to arc magmatism in the Andes of Central Chile. *Contrib. Mineral. Petrol.* **98**, 455–489.

Hole, M.J., Saunders, A.D., Marriner, G.F. and Tarney, J. (1984): Subduction of pelagic sediments: implication for the origin of Ce-anomalous basalts from the Mariana Islands. *J. Geol. Soc. London* **141**, 453–472.

Hovorka, D. (1996): Mesozoic non-ophiolitic volcanics of the Carpathian Arc and Pannonian Basin. *Geologica Carpathica* **47**, 63–72.

Jackson, M.L. (1958): Soil chemical analysis. Prentice-Hall, 498 pp.

Kapezhinskas, P., McDermott, F., Defant, M.J., Hochstaedter, A., Drummond, M.S., Hawkesworth, C.J., Kolosov, A., Maury, R.C. and Bellon, H. (1997): Trace elements and Sr–Nd–Pb isotopic constraints on a three-component model of Kamchatka Arc petrogenesis. *Geochim. Cosmochim. Acta* **61**, 577–600.

Kay, S.M. and Kay, R.W. (1985): Aleutian tholeiitic and calc-alkaline magma series I: The mafic phenocrysts. *Contrib. Mineral. Petrol.* **90**, 276–290.

Kovacs, S. (1982): Problems of the "Pannonian Median Massif" and the plate tectonics concept. Contribution based on the distribution of Late Paleozoic – Early Mesozoic isopic zones. *Geol. Rundschau* **71**, 617–640.

Leake, B.E. (1978): Nomenclature of amphiboles. *Miner. Petrogr. Acta Bologna* **22**, 195–224.

Leterrier, J., Maury, R. C., Thonon, P., Girard, D. and Marchal, M. (1982): Clinopyroxene composition as a method of identification of the magmatic affinities of paleo-volcanic series. *Earth Planet. Sci. Lett.* **59**, 139–154.

Lupu, M., Antonescu, E., Avram, E., Dumitrica, P. and Nicolae, I. (1995): Comments on the age of some ophiolites from the north Drocea Mts. *Rom. Jour. Tect. Reg. Geol.* **76**, 21–25.

Miyashiro, A. (1974): Volcanic rock series in island arcs and active continental margins. *Am. J. Sci.* **274**, 321–355.

Nelson, S.T. and Montana, A. (1992): Sieve-textured plagioclase in volcanic rocks produced by rapid decompression. *Am. Mineral.* **77**, 1242–1249.

Nicolae, I. (1995): Tectonic setting of the ophiolites from the South Apuseni Mountains: magmatic arc and marginal basin. *Rom. Jour. Tect. Reg. Geol.* **76**, 27–38.

Nicolae, I., Soroiu, M. and Bonhomme, G.M. (1992): Ages K–Ar de quelques ophiolites des Monts Apuseni du sud (Roumanie) et leur signification géologique. *Géologie Alpine* **68**, 77–83.

Pana, D.I., 1998. Petrogenesis and tectonics of the basement rocks of the Apuseni Mountains: significance for the alpine tectonics of the Carpathian-Pannonian region. PhD thesis, Univ. of Alberta (Canada), Edmonton, 356 pp.

Pearce, J.A. (1983): Role of the sub-continental lithosphere in magma genesis at active continental margins. In: Hawkesworth, C. J. and Norry, M. J. (eds.): Continental basalts and mantle xenoliths. Shiva Publ. Co., Nantwich, 230–249.

Peccerillo, A. and Taylor, S.R. (1976): Geochemistry of Eocene calc-alkaline volcanic rocks from the Kastamonu area, northern Turkey. *Contrib. Mineral. Petrol.* **58**, 63–81.

Radulescu, D.P. and Sandulescu, M. (1973): The plate-tectonic concept and the geological structure of the Carpathians. *Tectonophysics* **16**, 155–161.

Romick, J.D., Kay, S.M. and Kay, R.W. (1992): The influence of amphibole fractionation on the evolution of calc-alkaline andesite and dacite tephra from the central Aleutians, Alaska. *Contrib. Mineral. Petrol.* **112**, 101–118.

Saccani, E., Nicolae, I. and Tassinari, R. (2001): Tectono-magmatic setting of the Jurassic ophiolites from the South Apuseni Mountains (Romania): petrological and geochemical evidence. *Ofioliti* **26**, 9–22.

Sandulescu, J. and Visarion, M. (2000): Crustal structure and evolution of the Carpathian-Western Black Sea areas. *First Break* **18**, 103–108.

Savu, H., Udrescu, C. and Neacsu, V. (1981): Geochemistry and geotectonic setting of ophiolites and island arc volcanics of the Mures zone (Romania). *Ofioliti* **6(2–3)**, 269–286.

Savu, H., Udrescu, C., Neacsu, V. and Ichim, M. (1994): Petrology and geochemistry of the effusive rocks from the ocean floor basalt complex in the Mures Zone. *Rom. Jour. Petrol.* **76**, 67–76.

Savu, H., Grabari, G. and Stoian, M. (1996): New data concerning the structure, petrology and geochemistry of the Late Kimmerian granitoid massif of Savarsin (Mures Zone). *Rom. Jour. Petrol.* **77**, 71–82.

Sisson, T.W. and Grove, T.L. (1993): Experimental investigation of the role of H_2O in calc-alkaline differentiation and subduction zone magmatism. *Contrib. Mineral. Petrol.* **113**, 143–166.

Sun, S.S. and McDonough, W.F. (1989): Chemical and isotopic systematics of ocean basalts: Implications for mantle composition and processes. In: Saunders, A.D. and Norry, M.J. (eds.): Magmatism in the Ocean Basins. *Geol. Soc. Spec. Publ.* **42**, 313–346.

Tsuchiayama, A. (1985): Dissolution kinetics of plagioclase in the melt system diopside-albite-anorthite, and origin of dusty plagioclase in andesites. *Contrib. Mineral. Petrol.* **89**, 1–16.

Wood, B.J. and Banno, S. (1973): Garnet-orthopyroxene and orthopyroxene-clinopyroxene relationships in simple and complex systems. *Contrib. Mineral. Petrol.* **42**, 109–124.

Zacher, W. and Lupu, M. (1998): The ocean floor puzzle of the Alpine-Carpathian orogenic belt. *Jahrb. Geol. Bundesanstalt (Wien)* **141**, 97–106.

Received 15 October 2001
Accepted in revised form 17 February 2003
Editorial handling: M. Engi